Canadian Mineralogist
Vol. 27, pp. 107-118 (1989)

EFFECT OF Al–Si DISTRIBUTION ON THE POWDER-DIFFRACTION MAXIMA OF ALKALI FELDSPARS AND AN EASY METHOD TO DETERMINE *T*1 AND *T*2 SITE OCCUPANCIES

GUY L. HOVIS
Department of Geology, Lafayette College, Easton, Pennsylvania 18042, U.S.A.

ABSTRACT

Extensive X-ray powder-diffraction data have been collected for alkali feldspar ion-exchange series spanning almost the whole range of physically accessible topochemically monoclinic Al–Si distributions. Analysis of the shifts of diffraction maxima as a function of composition, structure, and degree of Al–Si order reveals which peaks are most useful for the calculation of computer-refined unit-cell dimensions, and for the estimation of Al–Si distribution directly from X-ray data. Separation of the 060 and $\bar{1}13$ powder-diffraction maxima is highly sensitive to the state of Al–Si order and is independent of composition for specimens containing more than 70% potassium. The degree of Al–Si order (defined by *Z*, equal to twice the difference in the mole fraction of Al in the *T*1 *versus* the *T*2 tetrahedral position) for alkali feldspars ranging from highly disordered sanidine to ordered orthoclase can be determined as $Z = -4.207 + 1.587\,[2\theta_{060} - 2\theta_{\bar{1}13}]$ (assuming Cu$K\alpha$ radiation). With highly precise X-ray data, this equation can produce Al contents for the tetrahedral sites of an unstrained monoclinic feldspar that are within ±0.012 of those that would have been determined from a single-crystal structure refinement of the same specimen. Values of *Z* for alkali feldspars with less than 70% potassium may also be estimated from the 060 - $\bar{1}13$ separation, and graphical methods are provided for doing so.

Keywords: X-ray powder data, alkali feldspars, Al–Si order.

SOMMAIRE

Une banque très complète de données de diffraction X (méthode des poudres) est disponible pour les membres des séries d'échange ionique impliquant presque toutes les distributions de Al et de Si dans les feldspaths alcalins topochimiquement monocliniques qu'il est possible de synthétiser. Une analyse des déplacements de pics de diffraction en fonction de composition, structure, et degré d'ordre Al–Si définit quelles sont les raies les plus utiles pour le calcul par ordinateur des paramètres réticulaires, et pour une estimation de la distribution de Al et de Si à partir des données de diffraction X. La séparation angulaire des raies 060 et $\bar{1}13$ dépend fortement du degré d'ordre et semble indépendante de la composition pour tout feldspath contenant plus de 70% du terme potassique. Le degré d'ordre découle du paramètre *Z*, égal à deux fois la différence dans la fraction molaire de l'aluminium des positions *T*1 et *T*2; pour les feldspaths alcalins variant de sanidine désordonnée à orthose ordonnée, *Z* est égal à $-4.207 + 1.587\,[2\theta_{060} - 2\theta_{\bar{1}13}]$ (rayonnement Cu$K\alpha$). Avec des mesures de précision élevée, cette expression peut évaluer la répartition de Al entre les deux sites à coordinance tétraédrique dans un feldspath monoclinique sans contraintes à 0.012 près des résultats d'un affinement de la structure du même échantillon. La séparation des raies 060 et $\bar{1}13$ peut aussi servir à évaluer *Z* pour tout feldspath contenant moins de 70% du terme potassique, à l'aide d'une méthode graphique.

(Traduit par la Rédaction)

Mots-clés: données de diffraction X (méthode des poudres), feldspath alcalin, degré d'ordre Al–Si.

INTRODUCTION

Hovis (1986) reported on the variation of unit-cell dimensions and volumes as a function of both composition and Al-Si distribution for five alkali feldspar ion-exchange series. Four of the series are topochemically monoclinic, and range from a relatively ordered series based on an "adularia" parent feldspar to a highly disordered series based on analbite. The fifth is a highly ordered topochemically triclinic series based on Amelia low albite. Details on the parent materials used to make these series, and on the synthesis histories and chemical compositions of all series members, were presented in Hovis (1986).

Hovis (1986) emphasized the characterization of structural state and determination of mole fraction of $KAlSi_3O_8$ (N_{Or}) in alkali feldspars through computer-refined unit-cell dimensions based on X-ray powder-diffraction data. However, neither the actual X-ray data nor a discussion of their usefulness for determination of structural state were presented; it is the purpose of this paper to do so.

Because ion-exchange rates are rapid, and experimental temperatures are low relative to those required for disordering, members of feldspar ion-exchange series normally inherit the Al–Si distribution of the parent feldspar. In the present study, the constancy of Al–Si distribution across ion-exchange series was confirmed by back-exchanging certain intermediate members of the various series to produce potassium end-members whose unit-cell dimensions are compared with compositionally similar feldspars produced *via* direct potassium-exchange of the parent materials (Table 5 of Hovis 1986, and related dis-

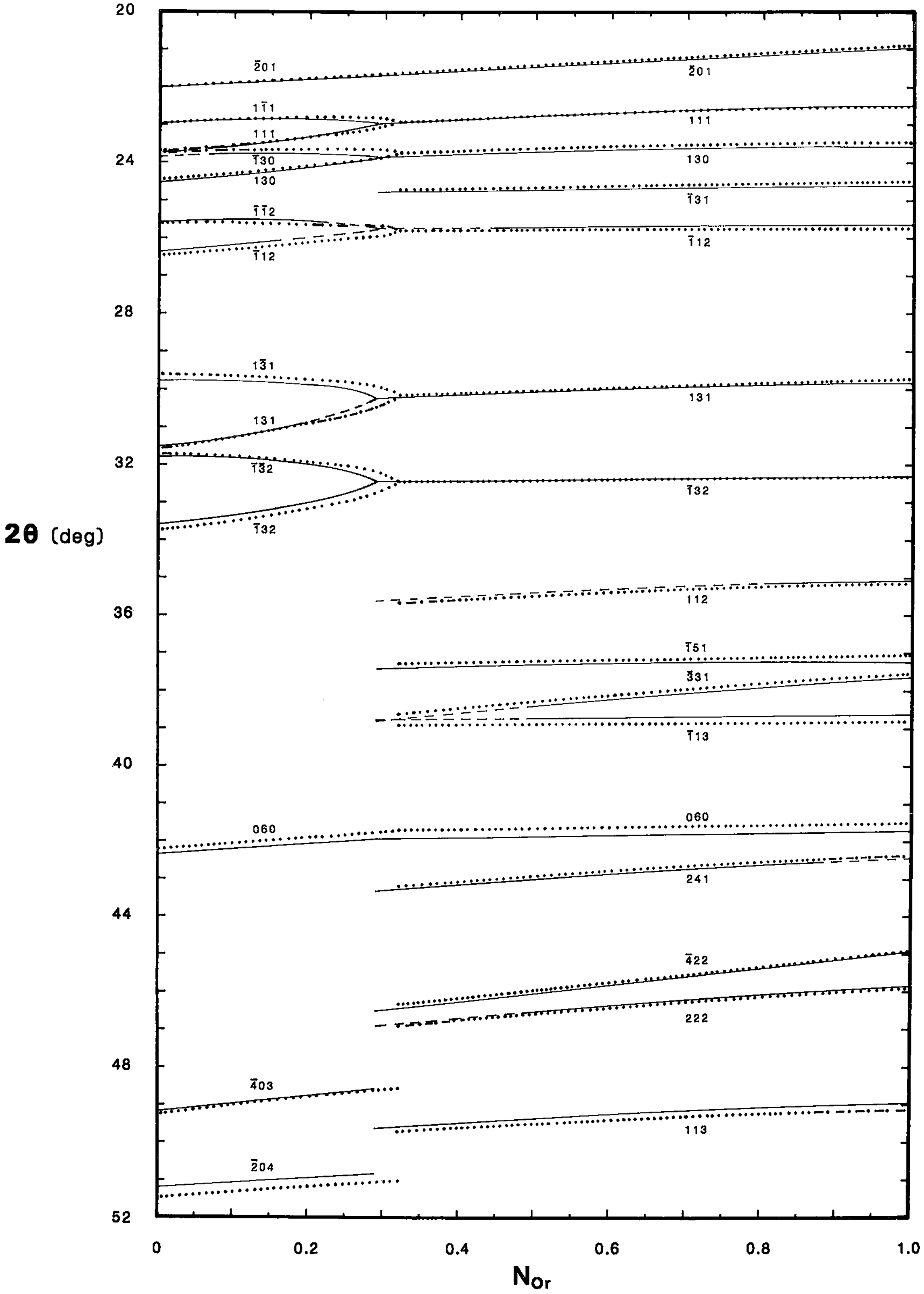
$\bar{2}01$
$1\bar{1}1$
111
$\bar{1}30$
130
$\bar{1}\bar{1}2$
$\bar{1}12$
$1\bar{3}1$
131
$\bar{1}\bar{3}2$
$\bar{1}32$
060
$\bar{4}03$
$\bar{2}04$
$\bar{2}01$
111
130
$\bar{1}31$
$\bar{1}12$
131
$\bar{1}32$
112
$\bar{1}51$
$\bar{3}31$
$\bar{1}13$
060
241
$\bar{4}22$
222
113
20
24
28
32
36
40
44
48
52
2θ (deg)
0
0.2
0.4
0.6
0.8
1.0
N_{Or}

cussion). By studying a number of ion-exchange series, therefore, it has been possible to separate the effects of Al–Si distribution from those of composition on both the X-ray and unit-cell dimension data.

As none of the parent feldspars used to synthesize these series is perthitic, the data reported here apply only to *unstrained* alkali feldspars. To avoid ambiguity the five series will be referred to by the names of their potassium end-members: high sanidine, Eifel sanidine, orthoclase, adularia, and microcline.

X-RAY METHODS

All feldspars were ground to fine powders and mixed with semiconductor-grade silicon (*a* was assumed to be 5.43054 Å: Parrish 1960), which was used as an internal standard in all of the X-ray work. Data were collected on a nonautomated Philips X-ray-diffraction system and Mark III data processor using nickel-filtered copper radiation and a scintillation detector. Scans were generally made over a 20° to 60° 2θ range at ¼°/min (chart speed: 1.25 cm/min). Most of the data reported are based on at least three such scans (see details in Hovis 1986, Table 6).

Differences in the positions of diffraction maxima used later in this paper to determine Al–Si distribution were also measured with a Scintag Pad V automated X-ray-diffraction system that employed a monochromator in the detection system. Values collected on the Scintag system are in good agreement with the manually measured data.

RESULTS

Identification of diffraction maxima for unit-cell refinements

It is not the purpose of this study to duplicate the powder-diffraction data previously given for disordered feldspars (Kroll *et al.* 1986, for sanidine – analbite crystalline solutions). Rather, my main aims are two-fold; firstly, I intend to show how Al–Si distribution *within topochemically monoclinic feldspars* relates to the positions of specific diffraction-maxima. The availability of data on four topochemically monoclinic alkali feldspar series that cover virtually the entire range of Al–Si distributions for such feldspars leads to a definitive statement on these relationships. Secondly, I wish to provide help in indexing powder patterns to those who have feldspars on which they want to perform full unit-cell refinements using computer programs such as those of Burnham (1962) and Appleman & Evans (1973).

X-ray data for topochemically monoclinic feldspars are presented in Figure 1, which shows the shifts of diffraction maxima from the most ordered to the most disordered feldspars (by solid and dotted lines, respectively) at all compositions. For investigators who do not know the Al–Si distributions of their feldspars, Figure 1 provides information on the maximum variations in peak positions due to Al–Si distribution. The figure thus is of value in identifying various peaks found on powder patterns. It differs from those given by other investigators in that *not all diffraction maxima are shown.* Included only are those peaks that are *useful* in performing unit-cell refinements, defined here as peaks free of interference from (not overlapped by) other peaks over extensive compositional ranges, and also having intensities sufficiently high that they are likely to be seen on an X-ray chart or "found" as peaks by peak-finder programs on automated systems. The only "overlapping" peaks plotted are those whose intensities exceed the intensities of interfering peaks by a ratio greater than 10:1.

As intermediate microline has not been studied, nor have its ion-exchange derivatives, no information is available on diffraction shifts for this mineral as a function of Al–Si distribution. Therefore, Figure 2 for topochemically triclinic feldspars applies only to low microcline – low albite crystalline solutions having near-perfect order. As with Figure 1, only peaks having no interference over extensive compositional ranges are shown.

Any feldspar will generate more peaks than are shown on Figures 1 and 2. Since some peaks have been intentionally omitted from these diagrams, investigators should use them with care. Comparison with Figures 2 and 3 of Kroll *et al.* (1986) and, for K-rich specimens, with Figure 2 of Blasi (1984), will be helpful. Note that even for the plotted peaks, data should not be used in compositional regions where the curves are dashed, or where interference from another (but in some cases unplotted) peak or set of peaks exists. Users of the diagrams must also take care not to misidentify diffraction maxima that are in the general vicinity of one or more other

FIG. 1. Positions of diffraction maxima for topochemically monoclinic alkali feldspars as a function of composition (N_{Or} is mole fraction $KAlSi_3O_8$) and Al–Si distribution. Solid lines are for the adularia series, dotted lines are for the high sanidine series. Data for the orthoclase and Eifel sanidine series plot between those of the other series. Only diffraction maxima for which there is little or no interference from other peaks over substantial compositional ranges are shown. Dashed portions of the plotted curves represent compositional regions in which there is interference from other (and in some cases unplotted) peaks. The 2θ values shown are for Cu$K\alpha$ radiation.

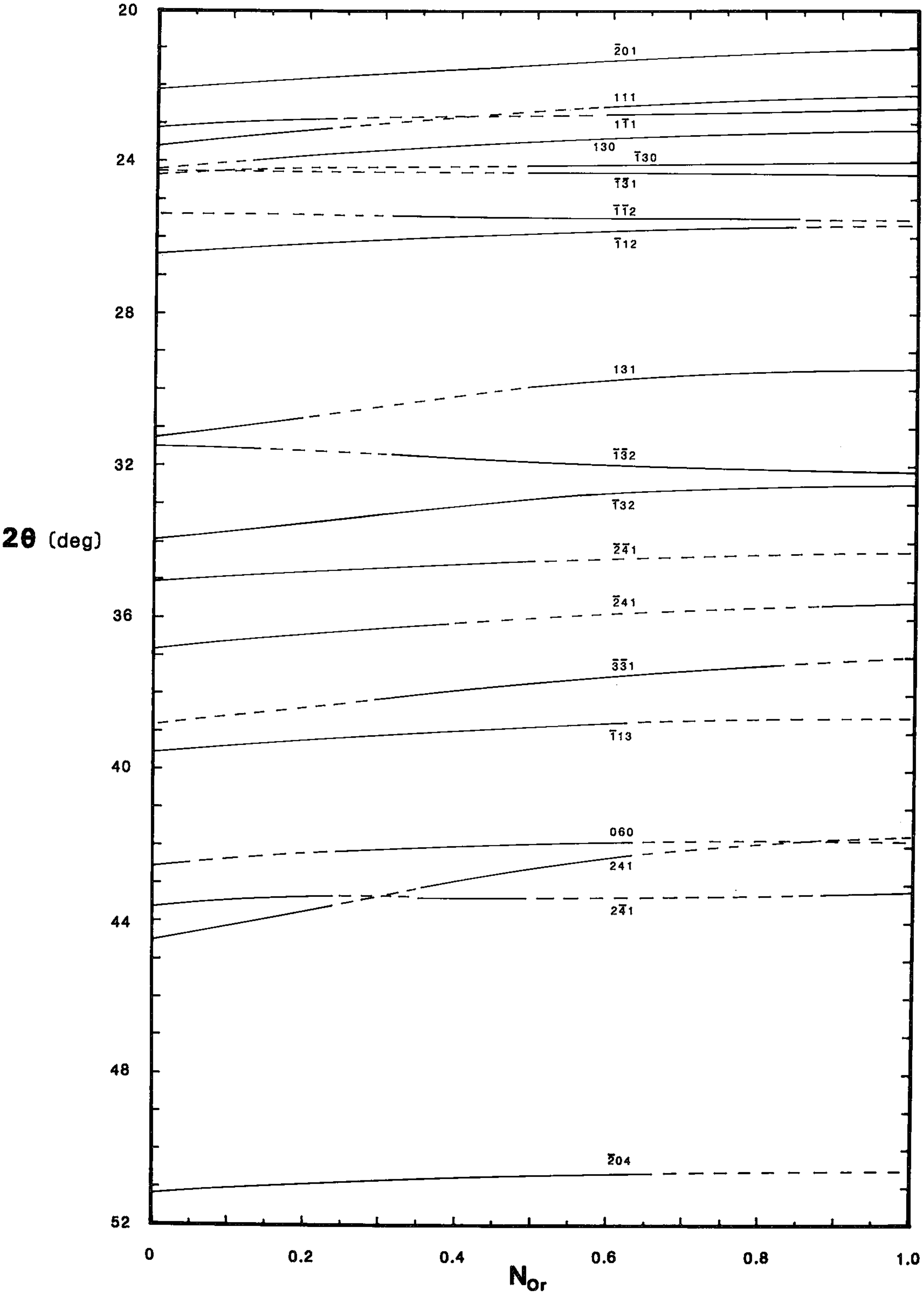
$\bar{2}01$
111
$1\bar{1}1$
130
$\bar{1}30$
$\bar{1}\bar{3}1$
$\bar{1}\bar{1}2$
$\bar{1}12$
131
$\bar{1}\bar{3}2$
$\bar{1}32$
$\bar{2}\bar{4}1$
$\bar{2}41$
$\bar{3}\bar{3}1$
$\bar{1}13$
060
241
$2\bar{4}1$
$\bar{2}04$
20
24
28
32
36
40
44
48
52
2θ (deg)
0
0.2
0.4
0.6
0.8
1.0
N_{Or}

unplotted peaks. In a few cases, the additional peaks may not overlap the peak of interest, but may be sufficiently near to cause confusion as to which peak is the one shown in the Figures.

A good example of the problems that can arise is illustrated by the 112 peak for K-rich monoclinic feldspars, which generally is found to have a higher value of 2θ than the $\bar{3}12$, 221 and $\bar{2}41$ peaks (not shown in Fig. 1), but nevertheless lies within 0.7°of them. For an unidentified feldspar, there might be a question as to which of the four is the 112 diffraction maximum. In such a case, the data for the peak in question are best ignored, although in some situations it is possible that enlargement of Figures 1 and 2 will help investigators to read the angles on the diagrams more accurately. The author will send single copies of enlarged versions of these Figures free of charge to interested investigators.

To use Figures 1 and 2, it is necessary first to determine the approximate composition of the feldspar in question, and also to ascertain whether it is topochemically monoclinic or triclinic. To determine composition, one should measure the position of the $\bar{2}01$ peak, which occurs at a 2θ value between approximately 20.95° and 22.05°. This value should be plotted both on Figures 1 and 2, and a line drawn for the appropriate composition through the data for all peaks at that composition. Then, from the sequence and exact positions of peaks along the plotted line, one can generally determine whether the feldspar has a topochemically monoclinic or triclinic Al–Si distribution. The 20° to 27° 2θ range is especially useful for this purpose. Note that feldspars that have two peaks in the region 20.95° to 22.05°, or that have a very broad single peak, are either perthitic or have a broad range of compositions. In these cases, the usefulness of Figures 1 and 2 will be limited.

As noted above, Figures 1 and 2 only include peaks that are useful over large compositional ranges. However, at any one composition there may be a significant number of additional peaks (that did not meet the criteria for inclusion in the plots shown here) that are free of interference and thus valuable for unit-cell refinements. In the general case, therefore, Figures 1 and 2 should be used to identify *useable* data. By inputting these "safe" data into an appropriate crystallographic program, one can perform a preliminary refinement of the unit-cell dimensions. From these preliminary values, one can then calculate the approximate positions of *all* peaks (including those not shown on Fig. 1 or 2) using the Bragg equation and the appropriate equation for interplanar spacings (*e.g.*, Azaroff & Buerger 1958, Chapter 6, Table 1). An appropriate list of the indices of peaks for which 2θ values should be calculated can be obtained from Borg & Smith (1969) for low albite, analbite (listed as "high albite"), low (= maximum) microcline, adularia, orthoclase, and sanidine (peaks for the last three being mostly the same). Using the calculated positions, additional peaks can be identified for use in a "final" refinement. It is wise to base the final refinement on multiple X-ray scans, preferably on equal numbers of forward and reverse scans, as the data can be slightly different for forward and reverse approaches to diffraction maxima. Data for preliminary refinements, however, may be based on a single scan.

Determination of Al–Si distribution from X-ray data

Wright (1968) proposed a "three-peak method" (later revised by Kroll & Ribbe 1987) for determination of the composition and structural state of an alkali feldspar from X-ray data, and also a "two-peak method" for determining structural state alone. Although the $\bar{2}01$ peak is an effective measure of composition and does not overlap other feldspar peaks at any value of N_{Or}, the 060 and $\bar{2}04$ peaks are not entirely free of interference. For low albite – microcline, the $\bar{2}04$ peak overlaps the 062, 043 and $\bar{4}41$ (as well as other) peaks at N_{Or} values above approximately 0.65, and thus is shown as a dashed curve in that compositional region on Figure 2. The 060 peak for these feldspars is associated with similar problems at both the sodium and potassium ends of the series.

For topochemically monoclinic feldspars, Figure 1 shows that although the 060 peak is suitable for use, the $\bar{2}04$ peak is overlapped by other peaks (such as $\bar{2}62$, 062, 043 and 350) over much of the monoclinic "segments" of the various series. It is only in the triclinic parts of these series that this peak is free of such interference. Indeed, plots of $\bar{2}04$ and $[2\theta_{\bar{2}04} - 2\theta_{060}]$ against composition clearly separate the various series into triclinic compositional regions (data for Cu$K\alpha$ radiation given in Table 1B and Fig. 3). Because these feldspars are not found in nature, however, the usefulness of the data is limited to synthetic specimens.

Although some of the peaks chosen by Wright (1968) potentially are problematic, the direct characterization of alkali feldspars from powder-diffraction data is very useful, especially for those who desire quick and easy estimates of composition and structural state, or for those who do not have the means

FIG. 2. Positions of diffraction maxima for the low microcline – low albite series. Only diffraction maxima for which there is little or no interference from other peaks over substantial compositional ranges are shown. Dashed portions of the curves indicate regions where there is interference from other peaks. The 2θ values are for Cu$K\alpha$ radiation.

TABLE 1A. SELECTED X-RAY POWDER DIFFRACTION DATA FOR MONOCLINIC MEMBERS OF TOPOCHEMICALLY MONOCLINIC ALKALI FELDSPAR SERIES STUDIED BY HOVIS (1986)

Monoclinic Feldspar	N_{Or}	$2\Theta_{\bar{2}01}$	$2\Theta_{\bar{3}31}$	$2\Theta_{\bar{1}13}$	$2\Theta_{060}$
High Sanidine Series					
7036	.9600	20.966	37.581	38.814	41.544
7060	.8074	21.117	37.803	38.815	41.550
8034	.7333	21.195	37.924	38.837	41.579
7058	.5993	21.336	38.138	38.849	41.597
7044	.4911	21.433	38.303	38.854	41.649
8008	.4406	21.493	38.400	38.877	41.673
7057	.3508	21.609	38.581	38.889	41.703
Eifel Sanidine Series					
7052	.9917	20.961	37.588	38.763	41.581
7002	.8359	21.094	37.783	38.774	41.583
8203	.7083	21.216	37.967	38.802	41.612
72001B	.5557	21.366	38.204	38.822	41.656
8202	.4346	21.497	38.414	38.837	41.693
Orthoclase Series					
7738	.9649	20.956	37.618	38.688	41.667
B18938	.9343	21.008	37.697	38.710	41.689
7814	.8719	21.058	37.770	38.711	41.690
7903	.7885	21.143	37.896	38.710	41.689
7908	.6981	21.233	38.034	38.736	41.716
7801	.5707	21.376	38.256	38.754	41.746
7905	.4652	21.497	38.455	38.780	41.801
7906	.3814	21.587	38.604	38.801	41.825
Adularia Series					
7045	.9972	20.963	37.656	38.630	41.746
7049	.9682	20.962	37.652	38.632	41.747
7198	.8602	21.072	37.812	38.653	41.753
7007	.8602	21.065	37.807	38.647	41.764
7918	.6776	21.261	38.102	38.667	41.801
7196C	.5365	21.407	38.329	38.681	41.819
7914	.4917	21.470	38.437	38.694	41.858
73013E	.3835	21.584	38.612	38.741	41.883

TABLE 1B. SELECTED X-RAY POWDER DIFFRACTION DATA FOR TRICLINIC MEMBERS OF TOPOCHEMICALLY MONOCLINIC ALKALI FEDLSPAR SERIES STUDIED BY HOVIS (1986)

Triclinic Feldspar	N_{Or}	$2\Theta_{\bar{2}01}$	$2\Theta_{060}$	$2\Theta_{\bar{2}04}$
High Sanidine Series				
7919	.2753	21.681	41.799	51.073
8001	.1510	21.813	41.972	51.255
7059	.1437	21.823	41.988	51.251
7015	.0099	21.985	42.186	51.452
Eifel Sanidine Series				
8201	.2898	21.663	41.776	50.998
72003	.1553	21.816	41.990	51.192
71102	.0032	21.980	42.215	51.400
Orthoclase Series				
7815	.3021	21.689	41.874	50.881
7818	.2376	21.763	41.969	50.977
7735	.1101	21.894	42.119	51.128
8431	.0135	22.022	42.300	51.289
Adularia Series				
7917	.2585	21.725	41.967	50.839
73011E	.2308	21.769	42.010	50.907
7927	.1879	21.793	42.077	50.961
7197	.0753	21.936	42.241	51.093
7190	.0103	22.023	42.336	51.175

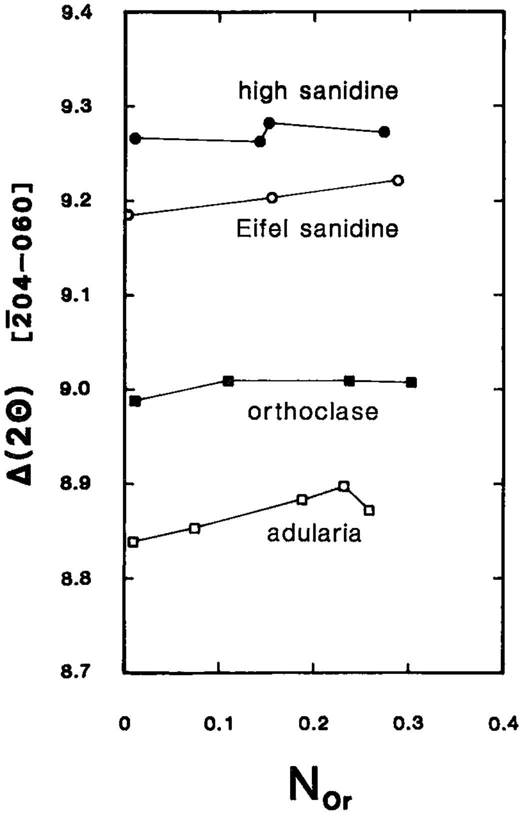

FIG. 3. Difference in 2θ for the $\bar{2}04$ and 060 diffraction maxima for triclinic members of the four topochemically monoclinic series of this investigation. As natural analogs of these feldspars do not exist, the diagram is useful only for synthetic specimens. The 2θ values here and in subsequent figures are for Cu*K*α radiation.

to determine cumputer-refined unit-cell dimensions.

To obtain highly precise Al–Si distributions, both diffraction maxima that shift substantially as a function of Al–Si distribution, and peaks that are free of interference at most K/Na values, are required. Furthermore, the use of differences in 2θ values, particularly between peaks that move in opposite directions as Al–Si distribution changes, is fruitful. As most data pertain to topochemically monoclinic feldspars, the methods developed here apply only to such feldspars.

Figure 1 reveals that three peaks in the 38° to 43° 2θ range are among the most sensitive diffraction-maxima to Al–Si distribution (peak positions assuming Cu*K*α radiation are given in Table 1A). Values (°2θ) decrease for the 060 and $\bar{3}31$ peak positions, and that of $\bar{1}13$ increases, as Al–Si distribution becomes disordered. Thus, plots of $[2\theta_{060} - 2\theta_{\bar{1}13}]$ and $[2\theta_{\bar{1}13} - 2\theta_{\bar{3}31}]$ *versus* composition (Figs. 4, 5)

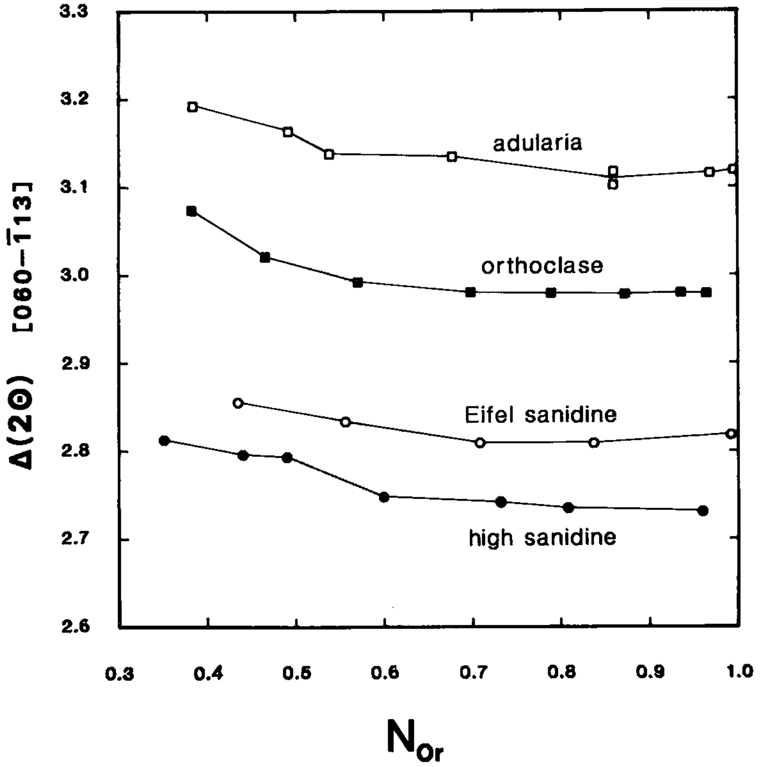

FIG. 4. Separation of the 060 and $\bar{1}13$ diffraction maxima for monoclinic members of the four topochemically monoclinic series. Because this parameter levels off with composition at N_{Or} values above approximately 0.7, it can be used to determine the Al–Si distribution of a relatively potassic feldspar, even if composition is not precisely known. Uncertainties in 2θ values here and in subsequent diagrams are ±0.01°. Values of N_{Or} are generally known to within 0.02.

clearly separate the various series. The difference between these differences, *i.e.*, the quantity $[2\theta_{060} + 2\theta_{\bar{3}31} - 2*2\theta_{\bar{1}13}]$ (Fig. 6), also works very well.

The plot of $[2\theta_{060} - 2\theta_{\bar{1}13}]$ *versus* N_{Or} is the most useful for characterization of structural state. This 2θ difference changes from 2.7°–2.8° in high sanidine to 3.1°–3.2°, in the adularia series. Furthermore, because the 2θ difference for each series is virtually constant at N_{Or} values above 0.7, it is not necessary to know the precise composition of a feldspar in order to apply the method. It is sufficient simply to know that the feldspar in question is relative potassic ($2\theta_{\bar{2}01}$ less than approximately 21.24°, assuming Cu$K\alpha$ radiation). Because most natural monoclinic feldspars with intermediate structural states have relatively potassic compositions, the 060–$\bar{1}$13 separation has wide application as a precise indicator of Al–Si distribution.

It has also been possible to successfully correlate values of $[2\theta_{060} - 2\theta_{\bar{1}13}]$ with specific Al–Si distributions, or values of Z, an ordering parameter for topochemically monoclinic feldspars given by Thompson (1969, 1970), where

$$Z \equiv 2\ [N_{Al,T1} - N_{Al,T2}] \qquad (1)$$

and N_{Al} is the mole fraction of aluminum in the designated tetrahedral site. To make this correlation, differences in 060–$\bar{1}$13 peak positions were calculated from cell-dimension data in the literature for all monoclinic potassium feldspars used in structure refinements. Values of Z based on bond-length data were calculated for the same feldspars using equations given by Kroll & Ribbe (1983; see Hovis 1986, Table 13 and related discussion). All data are given in Table 2 and shown in Figure 7, along with average values for potassic members of the four ion-exchange series used in this investigation. A linear least-squares fit to the single-crystal data produced the following relationship:

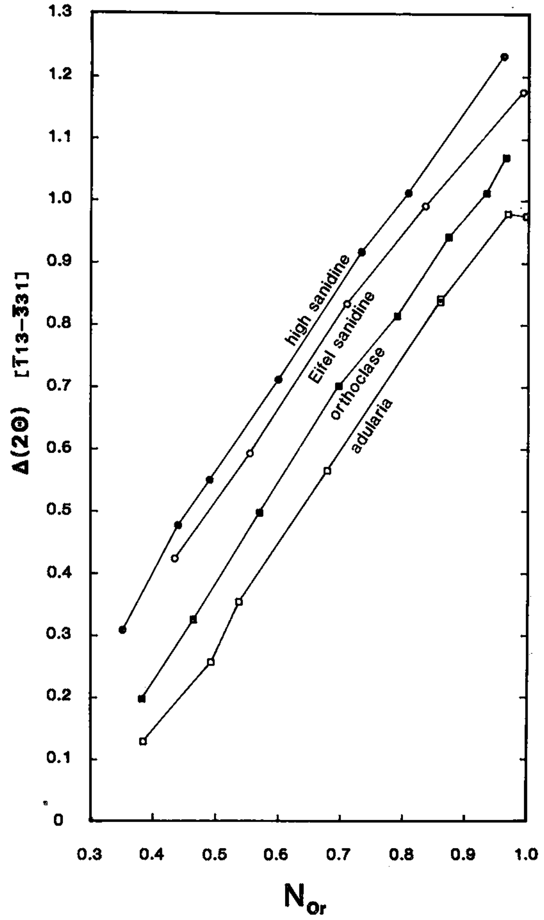

FIG. 5. Separation of the $\bar{1}13$ and $\bar{3}31$ diffraction maxima for monoclinic members of the four topochemically monoclinic series. This parameter clearly distinguishes the various series, but differences from series to series are less than for the parameters shown in Figures 4 and 6.

$$Z = -4.207(\pm 0.257) + 1.587(\pm 0.088)[2\theta_{060} - 2\theta_{\bar{1}13}] \quad (2)$$

with a standard error of 0.048. Significant figures beyond those justified by statistics have been given in order to avoid roundoff error. The standard error indicates that equation (2) (shown by the line in Fig. 7) is likely to produce a Z value for a particular feldspar that is within 0.048 of that which would have been obtained from a single-crystal refinement of its structure. This agreement results from uncertainties in the fraction of Al in each tetrahedral site on the order of ±0.012, reflecting only the statistics of the least-squares fit and *not* uncertainties in the bond-length equations of Kroll & Ribbe (1983).

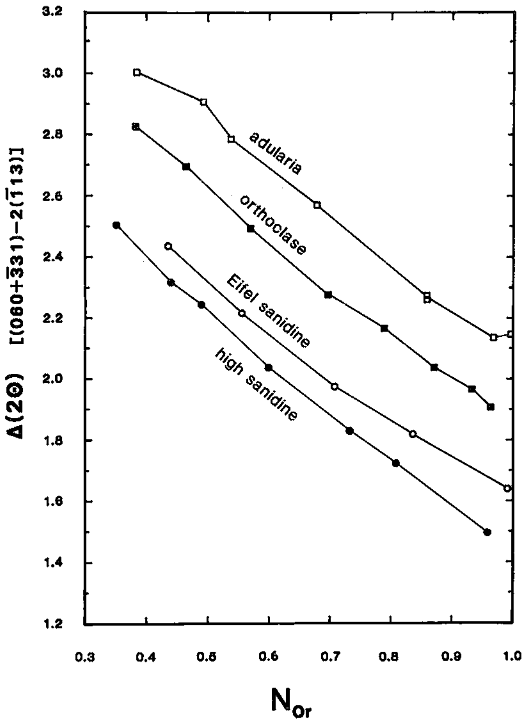

FIG. 6. The sum of 2θ values for the 060 and $\bar{3}31$ peaks minus twice the 2θ for the $\bar{1}13$ peak (equal to the *difference* between parameters shown in Figures 4 and 5) for monoclinic members of the four topochemically monoclinic series. Unlike the 060–$\bar{1}13$ separation, this parameter is strongly affected by K/Na value at all compositions. Thus, its application requires knowledge of N_{Or}.

TABLE 2. DATA USED TO DETERMINE RELATIONSHIPS EXPRESSED IN EQUATIONS (2) THROUGH (5), AND SHOWN IN FIGURES 7 AND 8

Monoclinic Feldspar	Ref.	Z	$\underline{c}_K$ (A)	$2\Theta_{060} - 2\Theta_{\bar{1}13}$
Annealed Eifel sanidine	1	0.072	7.1823	2.726
Annealed Spencer C	2,3	0.076	7.1780	2.723
High sanidine	4	0.113*	7.1802	2.738
Eifel sanidine 7002	5	0.196	7.1845	2.802
Eifel sanidine 7002	6	0.240	7.1852	2.761
Eifel sanidine 7002	7	0.308	7.1892	2.806
Eifel sanidine 7002	4	0.248*	7.1879	2.812
Eifel sanidine (not 7002)	1	0.280	7.1918	2.806
Spencer C	8	0.436	7.1965	2.931
Orthoclase	4	0.532*	7.2019	2.979
Spencer B	8	0.664	7.2108	3.103
Adularia 7007	5	0.704	7.2055	3.081
Adularia 7007	4	0.704*	7.2128	3.117
Himalaya orthoclase	9	0.820	7.2137	3.132

References: 1. Weitz 1972; 2. Cole et al. 1949; 3. Ribbe 1963; 4. Hovis 1974 and this investigation; 5. Phillips & Ribbe 1973; 6. Brown et al. 1974; 7. Ohashi & Finger 1974; 8. Colville & Ribbe 1968; and 9. Prince et al. 1973. Recent data of Blasi et al. (1987) and Scambos et al. (1987) became available too late for inclusion in the present work.

* Z values used for series studied during this investigation are as follows: Eifel sanidine, an average value based on references #5, 6, and 7; adularia from reference #5. High sanidine and orthoclase, values calculated from equation (15) of Hovis (1986) and based on the monoclinic members of those series for which $N_{Or} > 0.67$.

‡ All 2Θ values assume Cu K-alpha radiation.

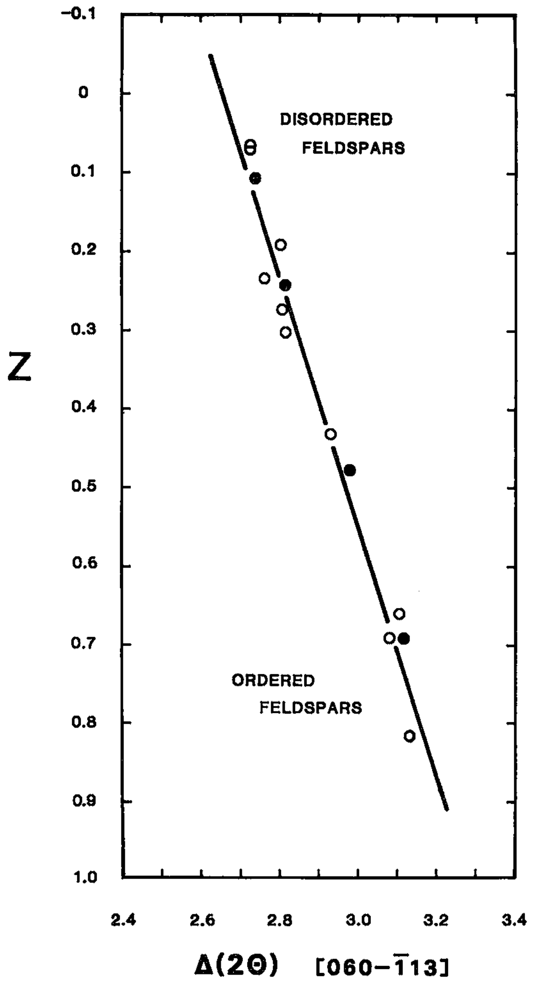

Fig. 7. Correlation of specific occupancies of the tetrahedral sites (expressed as Z, defined in the text) with separation of the 060 and $\bar{1}$13 peaks based on data for natural potassic feldspars used in single-crystal structural refinements (open circles; data in Table 2). Solid circles are average Z-values for K-rich members ($N_{Or} \geq 0.68$) of the four series of topochemically monoclinic feldspars used in this investigation. The solid line corresponds to equation 2. Although alkali feldspars are not likely to achieve negative values of Z, extension of the fitted line to such values is a reminder that ordering between $T1$ and $T2$ tetrahedral sites is nonconvergent.

As the mole fractions of aluminum in the two tetrahedral positions are simple functions of Z (Thompson 1969, 1970), it follows from equation (2) that these can be calculated as:

$$N_{Al,T1} = -0.802(\pm 0.067) + 0.3968(\pm 0.022)[2\theta_{060} - 2\theta_{\bar{1}13}] \quad (3)$$

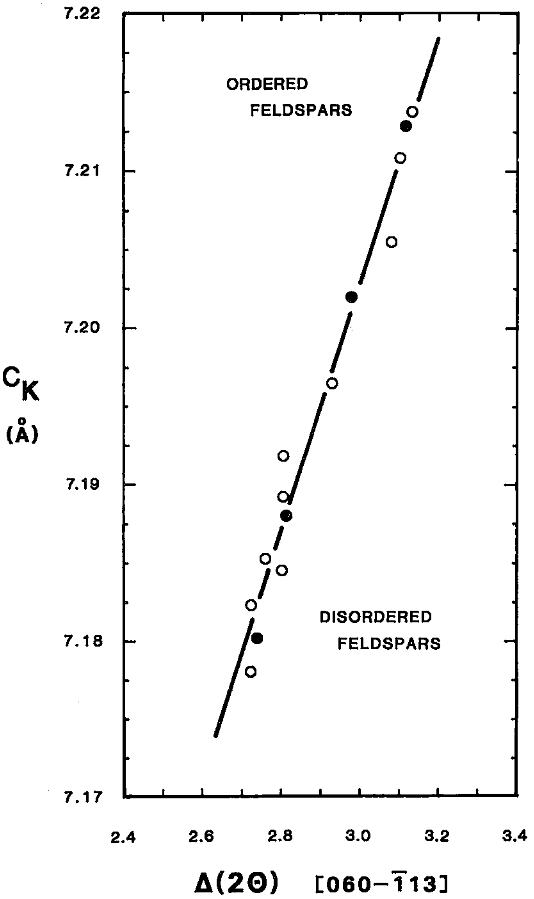

FIG. 8. Correlation of c_K (Hovis 1986; discussed in the text) with separation of the 060 and $\bar{1}$13 peaks. Open circles represent data for natural potassic feldspars used in single-crystal structural refinements (Table 2); solid circles are for the series of topochemically monoclinic feldspars used in this investigation. The solid line corresponds to equation 5.

and

$$N_{Al,T2} = +1.302(\pm 0.067) - 0.3968(\pm 0.022)[2\theta_{060} - 2\theta_{\bar{1}13}] \quad (4)$$

There is also a good correlation between $[2\theta_{060} - 2\theta_{\bar{1}13}]$ and c_K (Fig. 7), the physical Al-Si ordering parameter developed previously by Hovis (1986) based on the c unit-cell dimension of an alkali feldspar and its composition (N_{Or}). From a least-squares fit of data for monoclinic feldspars used in single-crystal structural refinements (Table 2), this relationship (Fig. 8) may be expressed as:

$$c_K = 6.9719(\pm 0.0125) + 0.0769(\pm 0.0043)[2\theta_{060} - 2\theta_{\bar{1}13}] \quad (5)$$

Figure 8 is a confirmation of the sensitivity of both c_K and $[2\theta_{060} - 2\theta_{\bar{1}13}]$ to Al–Si distribution; it also can be used in conjunction with equation (8) of Hovis (1986) to estimate the c cell dimension of an alkali feldspar ("c_{obs}") without a full unit-cell refinement.

Equation (2) will yield significant errors if applied to natural monoclinic feldspars that are substantially more sodic than $N_{Or} = 0.7$. The following equation (Fig. 9, raw data in Table 1A and 1B), based on $2\theta_{\bar{2}01}$ data for topochemically monoclinic feldspars studied by Hovis (1986), can be used to check the molar ratio K/(K+Na) in a natural feldspar whose composition is unknown:

$$N_{Or} = 70.726(\pm 9.973) - 5.6200(\pm 0.9295)\ 2\theta_{\bar{2}01} + 0.10936(\pm 0.02165)\ 2\theta^2_{\bar{2}01}] \quad (6)$$

Although many natural feldspars will have N_{Or} values greater than 0.7, certain samples of sanidine will produce compositions nearer the middle of the compositional range. Values of Z for these should be estimated graphically using Figure 4 by interpolat-

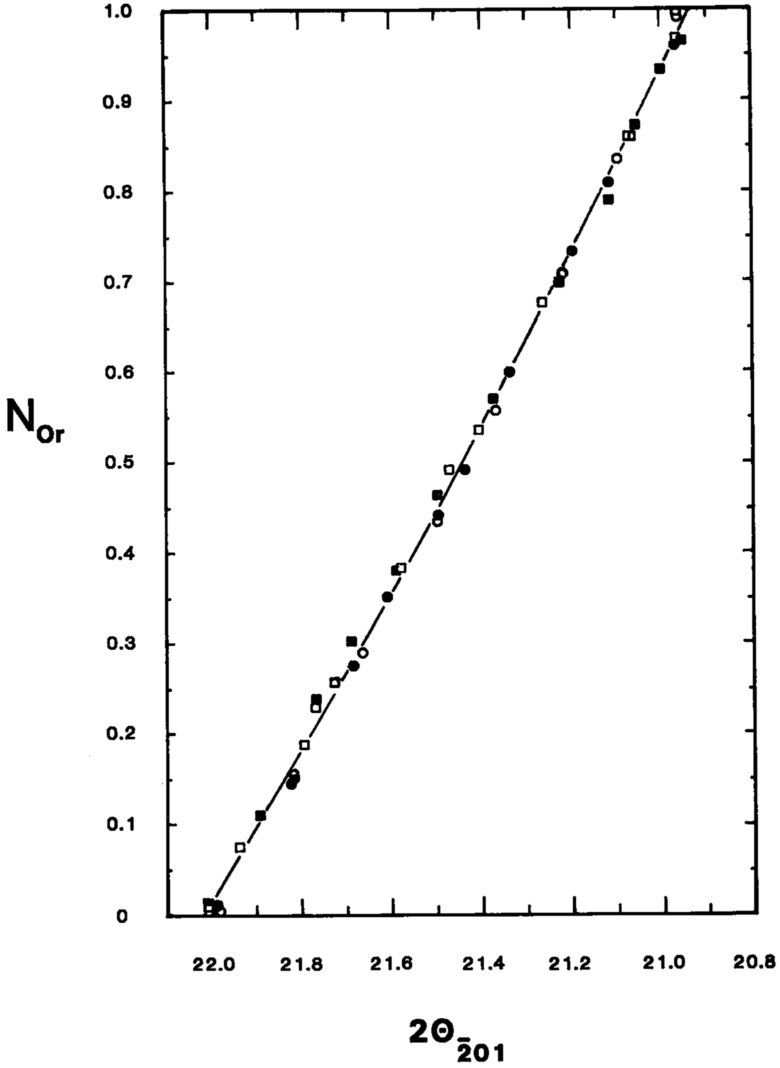

FIG. 9. Values of 2θ for the $\bar{2}01$ peak as a function of composition based on the four series of topochemically monoclinic alkali feldspars used in this investigation (solid circles, high-sanidine series; open circles, Eifel sanidine series; solid squares, orthoclase series; open squares, adularia series). The best least-squares fit to the data is slightly nonlinear, and is given by equation 6.

ing between feldspar series from Z values for the series given in Table 2.

SUMMARY AND CONCLUSIONS

Figures 1 and 2 give data that will be useful to investigators who wish to determine the Al–Si distributions of alkali feldspars *via* calculation of unit-cell dimensions. The diagrams, however, intentionally exclude diffraction maxima for which there is substantial interference from other peaks. Thus, it will be helpful to use these diagrams in conjunction with data provided by other investigators, *e.g.*, Borg & Smith (1969), Kroll & Ribbe (1983), Blasi (1984), and Kroll *et al.* (1986).

Equation (2) is provided for those wishing to characterize the Al–Si distributions of monoclinic alkali feldspars quickly without performing full unit-cell refinements. Because this method employs a *difference* in peak positions, it has the advantage of requiring no internal standard in the work. For accurate application, the feldspars in question should not be perthitic, nor have N_{Or} values substantially above 0.7.

Although the methods described furnish researchers with a quick and easy method to determine the Al–Si distributions and N_{Or} values of alkali feldspars, the estimates will only be as good as the data collected. Multiple passes in both forward and reverse directions at slow scan-rates are essential for maximum precision. Even so, this method will produce rapid determinations, facilitated by the close proximity of the 060 and $\bar{1}13$ peaks.

ACKNOWLEDGEMENTS

This research was supported by the National Science Foundation through grants EAR-8319084 and EAR-8616403, and through NSF College Science Instrumentation Grant CSI-8552030. I thank Jason Kelsey, who helped with X-ray measurements done on the automated Scintag Pad V X-ray-diffraction system. His participation in the work was partly supported through a Lafayette College summer student research grant. A. Blasi, P. Černý, R.B. Ferguson, J. L. Jambor and R.F. Martin provided helpful suggestions for improvement of this manuscript.

REFERENCES

APPLEMAN, D.E. & EVANS, H.T. (1973): Job 9214: indexing and least-squares refinement of powder diffraction data. *U.S. Geol. Surv. Comput. Contrib.* **20** (*NTIS Doc.* **PB2-16188**).

AZAROFF, L.V. & BUERGER, M.J. (1958): *The Powder Method in X-ray Crystallography.* McGraw-Hill, New York.

BLASI, A. (1984): The variation of 2θ angles in powder diffraction patterns of one and two-step K-rich feldspars. *Bull. Minéral.* **107**, 437-445.

______, DE POL BLASI, C. & ZANAZZI, P.F. (1987): Structure refinement of a high sanidine produced by dry annealing a Bedford low microcline for 200 days at 1050°C. *Rend. Soc. Ital. Mineral. Petrol.* **42**, 325.

BORG, I.Y. & SMITH, D.K. (1969): Calculated X-ray powder patterns for silicate minerals. *Geol. Soc. Am. Mem.* **122.**

BROWN, G.E., HAMILTON, W.C. & PREWITT, C.T. (1974): Neutron diffraction study of Al/Si ordering in a sanidine: a comparison with X-ray diffraction data. *In* The Feldspars (W.S. MacKenzie & J. Zussman, eds.). Manchester Univ. Press, Manchester, England.

BURNHAM, C.W. (1962): Lattice constant refinement. *Carnegie Inst. Wash. Year Book* **61**, 132-135.

COLE, W.F., SORUM, H. & KENNARD, O. (1949): The crystal structures of orthoclase and sanidinized orthoclase. *Acta Crystallogr.* **2**, 280-287.

COLVILLE, A.A. & RIBBE, P.H. (1968): The crystal structure of an adularia and a refinement of the structure of orthoclase. *Am. Mineral.* **53**, 25-37.

HOVIS, G.L. (1974): A solution calorimetric and X-ray investigation of Al–Si distribution in monoclinic potassium feldspars. *In* The Feldspars (W.S. MacKenzie & J. Zussman, eds.). Manchester Univ. Press, Manchester, England.

______ (1986): Behavior of alkali feldspars: crystallographic properties and characterization of composition and Al-Si distribution. *Am. Mineral.* **71**, 869-890.

KROLL, H. & RIBBE, P.H. (1983): Lattice parameters, composition, and Al, Si order in alkali feldspars. *In* Feldspar Mineralogy (2nd edition, P.H. Ribbe, ed.). *Mineral. Soc. Am., Rev. Mineral.* **2**, 57-99.

______ & ______ (1987): Determining (Al, Si) distribution and strain in alkali feldspars using lattice parameters and diffraction-peak positions: a review. *Am. Mineral.* **72**, 491-506.

______, SCHMIEMANN, I. & VON CÖLLN, G. (1986): Feldspar solid solutions. *Am. Mineral.* **71**, 1-16.

OHASHI, Y. & FINGER, L.W. (1974): Refinement of the crystal structure of sanidine at 25°C and 400°C. *Carnegie Inst. Wash. Year Book* **73**, 539-544.

PARRISH, W. (1960): Results of the I.U.Cr. precision lattice parameter project. *Acta Crystallogr.* **13**, 838-850.

Phillips, M.W. & Ribbe, P.H. (1973): The structures of monoclinic potassium-rich feldspars. *Am. Mineral.* **58**, 263-270.

Prince, E., Donnay, G. & Martin, R.F. (1973): Neutron diffraction refinement of an ordered orthoclase structure. *Am. Mineral.* **58**, 500-507.

Ribbe, P.H. (1963): A refinement of the crystal structure of sanidinized orthoclase. *Acta Crystallogr.* **16**, 426-427.

Scambos, T.A., Smyth, J.R. & McCormick, T.C. (1987): Crystal-structure refinement of high sanidine from the upper mantle. *Am. Mineral.* **72**, 973-978.

Thompson, J.B., Jr. (1969): Chemical reactions in crystals. *Am. Mineral.* **54**, 341-375.

______ (1970): Chemical reactions in crystals: corrections and clarification. *Am. Mineral.* **55**, 528-532.

Weitz, G. (1972): Die Struktur des Sanidins bei verschiedenen Ordnungsgraden. *Z. Kristallogr.* **136**, 418-426.

Wright, T.L. (1968): X-ray and optical study of alkali feldspar. II. An X-ray method for determining the composition and structural state from measurement of 2θ values for three reflections. *Am. Mineral.* **53**, 88-104.

Received February 16, 1988, revised manuscript accepted June 24, 1988.